Using of Broadened Asymmetric Waveguide Structure for 980nm Diode Laser

Seyed Peyman Abbasi* and Arash Hodaei

Semiconductor Laser Group, Iranian National Laser Center (INLC), Tehran, Iran

***Corresponding author email:** pabbasi2001@gmail.com

Regular paper: Received: Apr. 29, 2021, Revised: Dec. 26, 2021, Accepted: Dec. 28, 2021, Available Online: Dec. 30, 2021, DOI: 10.52547/ijop.15.2.125

ABSTRACT— Laser diode beam divergence is the main parameter for beam shaping and fiber optic coupling. Increasing the waveguide layer thickness is the conventional method to decrease the beam divergence. In this paper, the broadened asymmetric waveguide is introduced to decrease the divergence without increasing the optical power. The asymmetric waveguide was used to shift the vertical optical field to n-section, which has lower free carrier loss. The main target in this research is to minimize the internal loss to avoid the disadvantage of the broadened waveguide. Finally the beam divergence was decreased to 35 degrees that is very suitable for the conventional multi-mode optical fiber coupling and the optical power was increased to 2400mW in the laser diode with 100μm stripe width and 1mm cavity length. In addition to the fiber coupling, this improvement can be used for other direct applications that need beam shaping.

KEYWORDS: Asymmetric structure, Beam divergence, Cavity length, Internal loss, Laser diode.

I. INTRODUCTION

High power 980nm diode lasers are important for many direct applications and optical pumped sources such as fiber lasers. These applications require high optical output, high efficiency and small beam divergence, which prepare the high optical fiber coupling efficiency [1], [2]. But the low divergent beam needs a broadened waveguide. On the other hand, the broadened waveguide increases the threshold current that limits the optical power. As a result, these conflicting demands require a careful design of the diode structure with emphasis on the waveguide structure [1], [3].

High power diode lasers need a long cavity length. Increasing the cavity length, the internal optical loss must be decreased [4]. The free carrier loss is the main portion of the internal loss [5]. To use the long cavity structure, the free carrier loss must be minimized. Asymmetric waveguide structures can decrease the free carrier loss [6]–[8]. Therefore, an asymmetric non broadened waveguide structure was introduced to decrease the loss with increasing the refractive index of the n-cladding layer [6]. It is obvious that in an asymmetric structure, the vertical optical profile is moved to the n-cladding layer. The free carrier loss in n-section is lower than the p-section. Because the absorption cross section for an electron is 3-4 times lower than a hole. Some researchers used p-doping in the waveguide layer to improve the InGaAs/InGaAsP laser diode performance. In these structures the threshold current density is decreased to 150A/cm^2, and the internal loss was also decreased to 2.2cm^{-1} [7]. In another study, Ryvkin et al introduced low power asymmetric GaAs/AlGaAs with a doped barrier interlayer. The threshold current density and the beam divergence in this structure were 150A/cm^2 and 29 degrees respectively [8].

In this study, an InGaAs/AlGaAs symmetric structure was improved by an asymmetric structure. Three strategies were used for improvement. First, the waveguide layer broadened to decrease the vertical beam

divergence. Second, the n-waveguide layer thickness was increased more than p-waveguide layer, and also the aluminum mole fraction was decreased slightly (2%) in the n-cladding layer to increase the refractive index of the n-cladding layer. increasing the waveguide thickness and the refractive index change was limited by the mode number. The last strategy is using a carrier confinement layer to increase the internal quantum efficiency and as a consequence increase the slope efficiency.

II. THEORETICAL MODEL

A. *Internal Loss*

The internal losses are primarily controlled by the free-carrier light absorption. There are three main origins for the carrier absorption. The first one is the absorption in cladding layers which are doped with donors or acceptors. The second origin is the light absorption in the active region where the concentration of the non-equilibrium carriers is extremely high. The third origin is the light absorption in the undoped waveguide where non-equilibrium electrons and holes are injected to [9], [10]. The internal optical loss α_{int} in heterostructure lasers can be determined by the summation of losses α_i related to the free carrier absorption in all epitaxial layers in semiconductor lasers [5], [10]:

$$\alpha_{\text{int}} = \sum \alpha_i, \ \alpha_i = \Gamma_i \alpha_i^l , \tag{1}$$

where Γ_i is the optical confinement factor of each layer *i*. The optical loss coefficient, α_i^l, and optical confinement factor, Γ_i, are expressed by [10]:

$$\alpha_i^l = \sigma_n n + \sigma_p p , \tag{2}$$

$$\Gamma_i = \frac{\int_i E^2 dx}{\int_{-\infty}^{+\infty} E^2 dx} , \tag{3}$$

where σ_n and σ_p denote the electron and hole cross sections, respectively, n and p are the electron and hole densities, respectively, and E is the optical field.

The electron and hole absorption cross sections are determined by [10]:

$$\sigma_n = \frac{q^3 \lambda^2}{4\pi \mu_n m_n^2 N_r \varepsilon_0 c^3} , \tag{4}$$

$$\sigma_p = \frac{q^3 \lambda^2}{4\pi \mu_p m_p^2 N_r \varepsilon_0 c^3} , \tag{5}$$

where q is the electron charge, λ is the photon wavelength, μ_n and μ_p are the electron and hole mobilities, respectively, and m_n and m_p are the effective masses of electrons and holes. N_r is the refractive index of the material, ε_0 is the electric constant and c is the velocity of light in vacuum.

It is noted that the optical confinement factor is related to the thickness and refractive index of layers. The optical confinement factor of the active layer determines the threshold current and total optical power. The maximum achievable optical power P_{CWMax} is determined by [11]:

$$P_{CWMax} = \frac{d}{\Gamma} W \frac{1 - R_f}{1 + R_f} P_{COMD} , \tag{6}$$

where d and Γ represent the thickness and the confinement factor of the active layer, respectively, W is the stripe width, and R_f is the front mirror reflectivity (output mirror) and P_{COMD} is catastrophic optical mirror damage level that is determined experimentally for different active layer materials and can be found in [11], [12].

B. *Waveguide*

The thicknesses and refractive indices of the waveguide and n- and p-cladding layers in an asymmetric structure are determined by the mode number and the confinement factor. The analysis of the mode number in the waveguide is explained in [13]. The asymmetric parameter,

a and the normalized frequency, V are determined as follows [13]:

$$a = \frac{n_{ncladd}^2 - n_{pcladd}^2}{n_{WG}^2 - n_{ncladd}^2}, \quad (7)$$

$$V = kd_{WG}\sqrt{n_{WG}^2 - n_{ncladd}^2}, \quad (8)$$

where n_{ncladd} and n_{pcladd} denote refractive indices of the n- and p-cladding layer, respectively. n_{WG} and d_{WG} are the refractive index and the thickness of the waveguide layer, respectively. In cutoff condition, it is clear that m modes may be supported by the asymmetric waveguide if V is between $m\pi + \tan^{-1}\sqrt{a}$ and $(m+1)\pi + \tan^{-1}\sqrt{a}$ [13].

III. Laser Structure and Simulation

Our laser diode structure was simulated by PICS3D. The simulation used k.p method for the band structure calculation in the active region. For validation, results of the fabricated symmetric structure laser diode in INLC, was also simulated. Double heterostructure epitaxial layers of a laser diode are listed in Table 1.

The laser diode in this study, is a single chip with a geometrical dimension of 500µm width and 1000µm cavity length. The stripe width of the laser is 100µm. The front and rear laser mirror reflectivities are 5% (single Al_2O_3 layer) and 95% (four pairs of Si and Al_2O_3 layers), respectively. The SiO_2 layer (insulator layer) was utilized to confine the injection current laterally (Fig. 1).

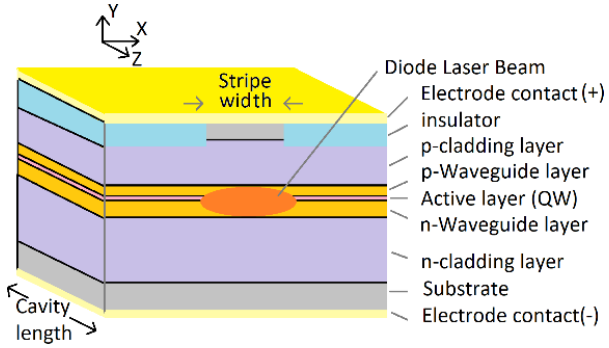

Fig. 1. Schematic view of a laser diode.

The laser diode chip was mounted on a Cu heat sink and packaged in TO-3 packaging model. The laser diode heat sink temperature (T=293K) was controlled by a thermoelectric controller (TEC).

Table 1. Laser diode epitaxial layers of the symmetric structure

Cap layer: p-GaAs 200nm
p-cladding layer: p-$Al_{0.38}Ga_{0.62}As$ 500nm
p-waveguide: p-$Al_{0.24}Ga_{0.76}As$ 400nm
Active layer QW: InGaAs
n-waveguide: n-$Al_{0.24}Ga_{0.76}As$ 400nm
n-cladding layer: n-$Al_{0.38}Ga_{0.62}As$ 500nm
Substrate: GaAs

For comparison, Experimental and simulation current-power (L-I) results are shown in Fig. 2 The results of the simulation have a good agreement with experimental results.

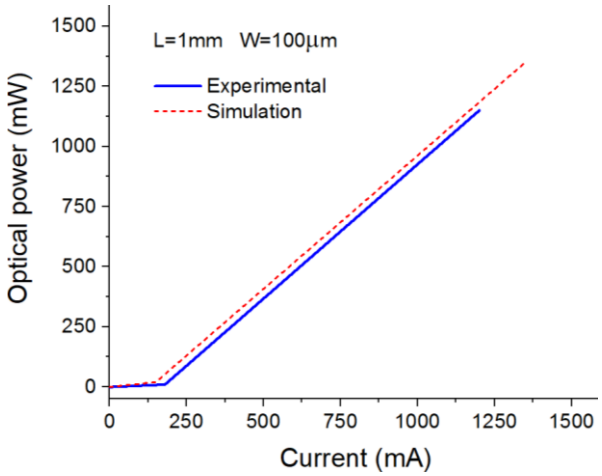

Fig. 2. Comparison of the experimental and simulation of the light-current characterization in the symmetric structure. The front and rear facet reflectivities are 5% and 95%, respectively. The characterization temperature is 300ºK.

IV. Asymmetric Structure

The broadened asymmetric waveguide structure was utilized to increase the vertical beam spot size (near field) and so to decrease the vertical beam divergence. In the asymmetric structure the active region is embedded in an $Al_{0.05}Ga_{0.95}As$ waveguide that is sandwiched between $Al_{0.33}Ga_{0.67}As$ and $Al_{0.30}Ga_{0.70}As$ p- and n-cladding layers, respectively. The refractive index n and the bulk band gap E_g in $Al_xGa_{1-x}As$ material are calculated from [14]:

$$n = \sqrt{13.1 - 3.05x}\,, \tag{9}$$

$$E_g = 1.424 + 1.277x\,, 0 < x < 0.4 \tag{10}$$

where x is the Al mole fraction. The effective mass and the mobility of the electron and hole for $Al_xGa_{1-x}As$ was estimated from experimental data in [14], [15]. The light absorption cross sections of the electron and hole are shown in Fig. 3. There are sharp peaks in the electron cross section at $0.4 < x < 0.5$. Therefore, the lower aluminum mole fraction $(x < 0.4)$ is suitable to minimize the absorption cross section and also to decrease the internal loss of the laser diode. Furthermore, in the cladding layer that is doped up to $10^{18}cm^{-3}$, the cross section becomes several times larger than undoped AlGaAs (like the waveguide layer).

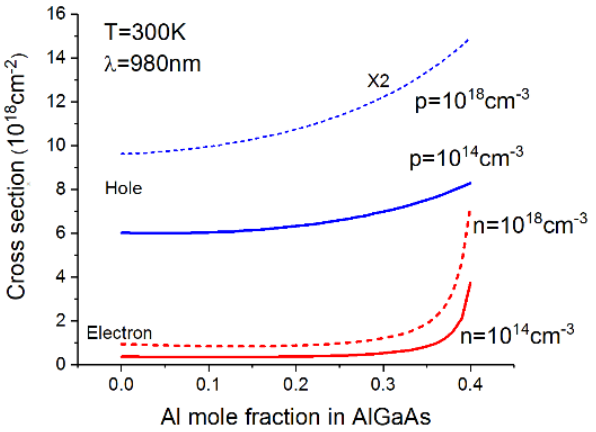

Fig. 3. Light absorption cross sections of the electron and hole for undoped AlGaAs (solid line) and doped AlGaAs (dashed line). The cross section for the hole in doped condition must be multiplied by 2.

Reducing the Al mole fraction decreases the band gap and increases the refractive index. The refractive index profile of both structures are compared in Fig. 4. The Al mole fraction of the waveguide was decreased, in the asymmetric structure, to increase the refractive index. The n-cladding layer refractive index is more than that of p-cladding layer and the thickness of n-waveguide is larger than p-waveguide. These changes shift the optical field to n-section and decrease the free carrier loss. The waveguide thickness and the refractive index selection support only the first vertical mode (fundamental).

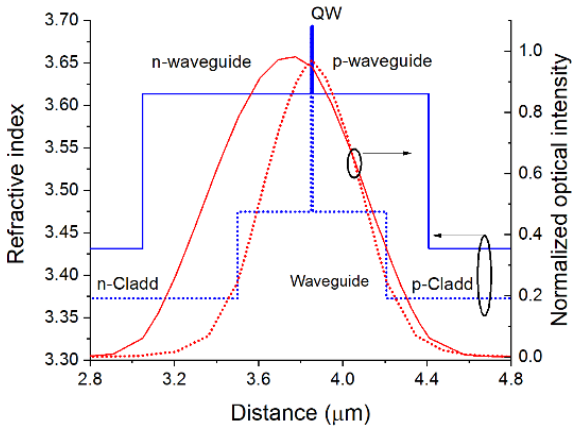

Fig. 4. Refractive index profile and optical field profile in the symmetric structure (dotted line) and the asymmetric structure (solid line). The confinement factors in active layer are 1.41% and 0.91% for the symmetric and asymmetric structures, respectively.

The model-solid theory is often employed to estimate the band edge offsets at heterointerfaces [10]. There are high carrier densities in the waveguide and cladding layer interfaces in n- and p-section. The overlap of the high carrier density and the optical field produces the free carrier loss and increases the internal loss. Figure 5 shows the band diagram of the symmetric and asymmetric structures. Changing the material in the waveguide and cladding layer and also increasing the waveguide thickness, the overlap of the optical field and carrier densities can be decreased.

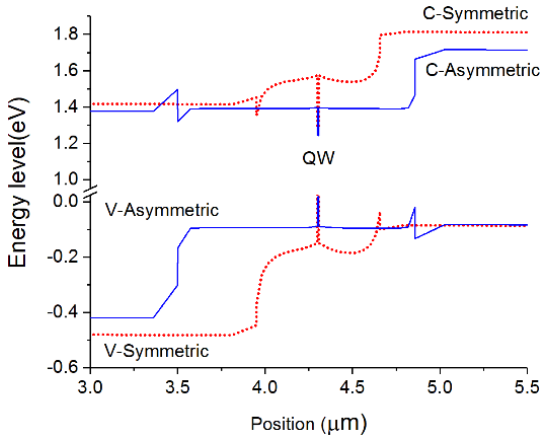

Fig. 5. Band diagram of the symmetric (dotted line) and asymmetric structure (solid line). The band edge offsets heterointerfaces of waveguide and cladding layer are shown.

The vertical optical field and the carrier density of two structures in the threshold current are shown in Fig. 6. In the asymmetric structure,

the overlap of the optical field with the hole carrier concentration is decreased. The overlap of the optical field and the free carrier loss are estimated by Eq. (2) and (3). The loss in each layer and the total loss is listed in Table 2. The optical loss in the asymmetric structure is decreased about 40%.

Table **2** Internal loss for two Laser diode structures.

Layer	Symmetric		Asymmetric	
	Loss(cm^{-1})	%	Loss(cm^{-1})	%
n-cladd.	0.130	5	0.015	2
n-WG	0.991	38	1.067	68
p-WG	1.414	54	0.431	28
p-cladd.	0.073	3	0.015	2
Total loss	2.61 cm^{-1}		1.54 cm^{-1}	

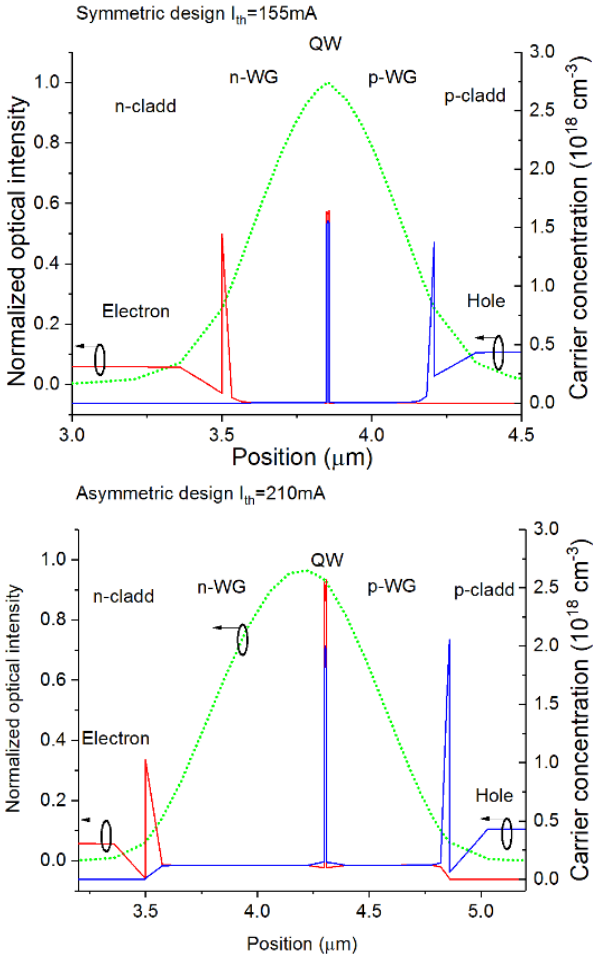

Fig. 6. Vertical optical field and the carrier density of the symmetric structure (top) and the asymmetric structure (bottom) in the threshold current. The red and blue lines show the electron and hole densities, respectively. The semi Gaussian green line is the profile of the optical field.

V. RESULTS

A. *Laser Characteristics*

The internal loss and the vertical mode number calculated in the pervious section, was utilized in the simulation. Lower optical confinement in the asymmetric structure causes higher achievable optical power. Figure 7 shows the electro-optical characteristics for two structures. The slope efficiency (SE) and power conversion efficiency (PCE) in the asymmetric structure are higher than the symmetric structure. And also the threshold current in the symmetric structure is lower because the waveguide thickness is thinner than the asymmetric structure. The far field profiles of two structures are shown in Fig. 8. In comparison with the symmetric structure, the beam divergence in the asymmetric structure was decreased 15% that is the main target in this research. The laser diode characteristics are listed in Table 3.

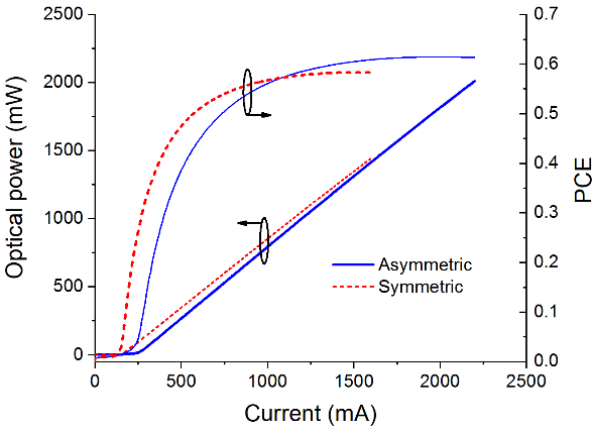

Fig. 7. Light-current (L-I) and the power conversion efficiency (PCE) characterization of the symmetric structure (dashed line) and the asymmetric structure (solid line).

Table **3** Laser diode characteristics of the symmetric and asymmetric structure with L=1mm.

parameters	**Unit**	**Sym.**	**Asym.**
Optical power	mW	2500	3100
Threshold current	mA	155	210
PCE	%	58	62
Slope efficiency	W/A	1.00	1.02
Series resistance	mΩ	78	63
divergence	degree	42	35

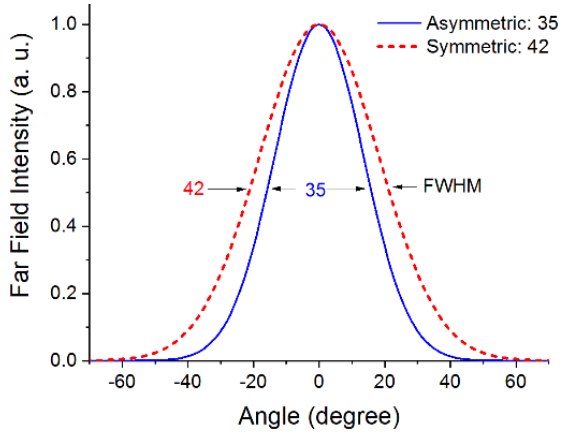

Fig. 8. Vertical far field (fast axis) profile of symmetric structure (dashed line) and asymmetric structure (solid line).

The laser emission wavelength and the active layer temperature for both the symmetric and asymmetric structures are shown in Fig. 9 and 10, respectively. The results show that the wavelength shift for the asymmetric structure is lower than the symmetric structure. On the other hand, the asymmetric structure has a better wavelength stability.

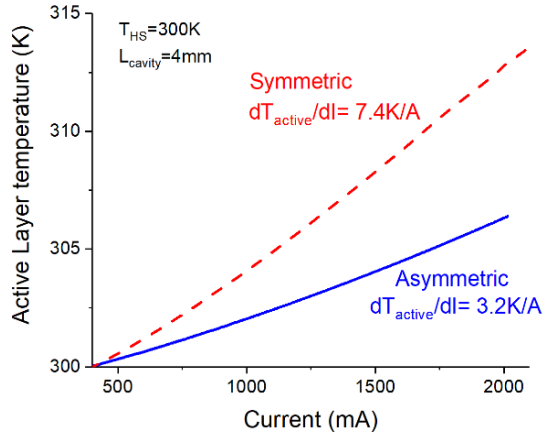

Fig. 9. Active layer temperature vs. current of th symmetric structure (dashed line) and the asymmetric structure (solid line).

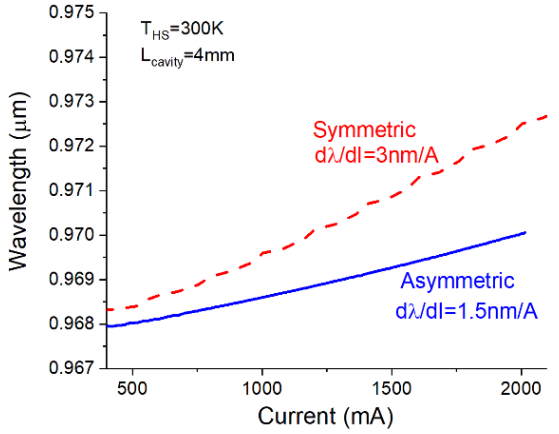

Fig. 10. The laser diode emission wavelength vs. current of the symmetric (dashed line) and the asymmetric structure (solid line).

B. *Internal Loss and IQE*

External Differential quantum efficiency η_d is calculated from the slope efficiency of the laser diode [2]:

$$\eta_d = \frac{\lambda q}{hc}\frac{dP(I)}{d(I)}, \tag{11}$$

where h is Planck's constant, $P(I)$ is the output optical power and I is the injection current. The internal quantum efficiency (IQE) η_i and the internal optical loss α_i are calculated from [2]:

$$\frac{1}{\eta_d} = \frac{1}{\eta_i} + \frac{\alpha_i}{\eta_i}\frac{1}{\ln\left(\frac{1}{R_f R_r}\right)}L, \tag{12}$$

where L and R_r denote the cavity length and the rear mirror reflectivity, respectively. The inverse External Differential quantum efficiency in deferent laser cavity lengths (1, 2 and 4mm) is shown in Fig. 11. The results show that the internal losses are 2.61cm^{-1} and 1.51 cm^{-1} for the symmetric and asymmetric structures, respectively. Furthermore IQE is 0.89 for both structures.

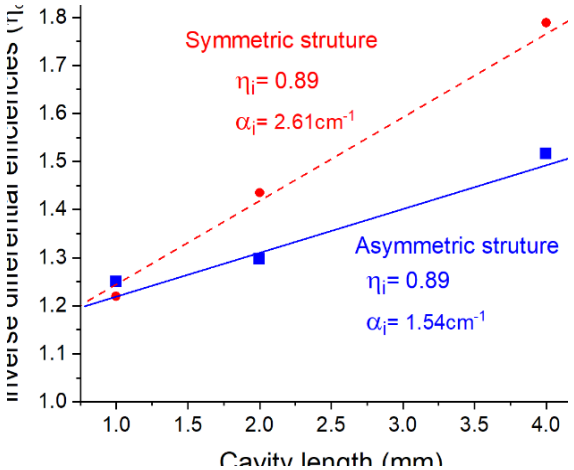

Fig. 11. Differential efficiency of the symmetric (dashed line) and asymmetric structures (solid line) in different cavity length to calculate the internal quantum efficiency and the internal optical loss.

C. *Cavity Length*

The threshold current density of the laser diode with different cavity lengths is shown in Fig. 12. The threshold current density is decreased with the cavity length. Furthermore, the results show that in long cavity devices the difference between threshold current densities for both structures is lower than that of the short cavity. In long cavity length devices, the asymmetric structure have higher achievable optical power because this structure can support higher optical power load on the front mirror.

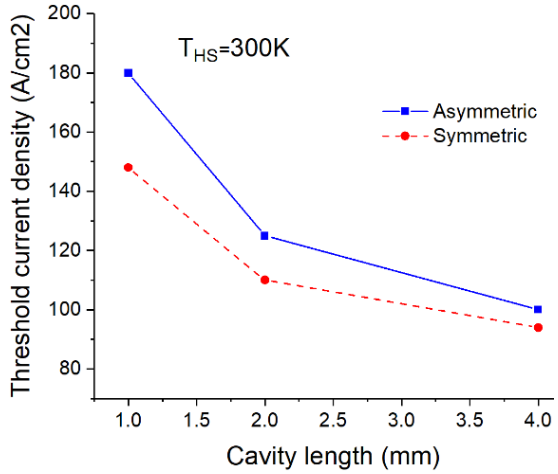

Fig. 12. Threshold current density for different cavity lengths of the symmetric (dashed line) and the asymmetric structure (solid line).

Finally the LIV laser diode characteristics for different cavity lengths in the asymmetric structure is shown in Fig. 13. With L=4mm the power conversion efficiency is 55%. Furthermore the series resistance in the long cavity length laser diodes is lower than that of the short cavity length lasers.

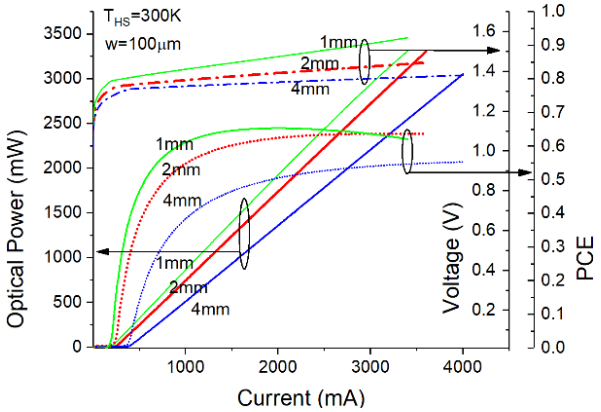

Fig. 13. Light-current (L-I), Voltage-current (V-I) and power conversion efficiency (PCE) characterization of the asymmetric structure in different cavity lengths.

VI. CONCLUSION

In this paper we introduced the broadened asymmetric waveguide structure for 980nm InGaAs/AlGaAs laser diode. The main target of this paper is decreasing the vertical beam divergence and the internal optical loss. The results showed that by using the proposed structure, the internal loss and the vertical beam divergence can be decreased up to 1.51 cm^{-1} and 35 degrees, respectively. Furthermore PCE and SE were increased in the asymmetric structure. The asymmetric structure was used to avoid the disadvantage of broadened waveguide. It's concluded that in long cavity length devices, the broadened asymmetric waveguide can be used to achieve the higher optical power without any significant increase in the threshold current.

REFERENCES

[1] A. Malag, E. Dabrowska, M. Teodorczyk, G. Sobczak, A. Kozłowska, and J. Kalbarczyk, "Asymmetric Heterostructure with Reduced Distance from Active Region to Heatsink for 810-nm Range High-Power Laser Diodes," IEEE J.Quantum Electron. Vol. 48, No. 4, pp. 465-471, 2012.

[2] R. Diehl, *High Power Diode Lasers*, New York, Springe, Ch. 2, 2000.

[3] B.S. Ryvkin and E.A. Avrutin, "Asymmetric, nonbroadened large optical cavity waveguide structures for high-power long-wavelength semiconductor lasers," J. Appl. Phys. Vol. 97, No. 6, pp. 123103 (1-7), 2005.

[4] B. Mroziewicz, *Physics of Semiconductor Lasers*, Warszawa, PWN, ch. 5, 1991.

[5] N.A. Pikhtin, S.O. Slipchenko, Z.N. Sokolova, and I.S. Tarasov "Internal Optical Loss in Semiconductor Lasers," Semiconductors, Vol. 38, No. 3, pp. 360–367, 2004.

[6] J.J. Lee, L.J. Mawst, and D. Botez, "Improved-performance, InGaAs=InGaAsP (λ =980 nm) asymmetric broad-waveguide diode lasers via waveguide-core doping," Electron. Lett. Vol. 39, No. 17, pp. 1250-1252, 2003.

[7] B.S. Ryvkin, E.A. Avrutin, and J.T. Kostamovaara, "Narrow versus broad

asymmetric waveguides for single-mode high-power laser diodes," J. Appl. Phys. Vol. 114, pp. 013104 (1-4), 2013.

[8] B.S. Ryvkin and E.A. Avrutin, "Improvement of differential quantum efficiency and power output by waveguide asymmetry in separate-confinement-structure diode lasers," IEE Proc.-Optoelectron., Vol. 151, No. 4, August 2004.

[9] B.S. Ryvkin and E.A. Avrutin, "Effect of carrier loss through waveguide layer recombination on the internal quantum efficiency in large-optical-cavity laser diodes," J. Appl. Phys. Vol. 97, pp. 113106 (1-6), 2005.

[10] K.A. Bulashevich1, V.F. Mymrin, S. Yu Karpov, D.M. Demidov and A.L. Ter-Martirosyan, "Effect of free-carrier absorption on performance of 808 nm AlGaAs-based high-power laser diodes," Semicond. Sci. Technol. Vol. 22, pp. 502–510, 2007.

[11] D. Botez, "High-Power Al-free Coherent and Incoherent Diode Lasers," in Conference Proceedings, LEOS'98, 11th Annual Meeting, 1998.

[12] P.G. ELISEEV, "Optical Strength of Semiconductor Laser Materials," Prog. Quant. Electr. Vol. 20, No. I, pp. 1-82, 1996.

[13] Chin-Lin Chen, *Foundations for Guided-Wave Optics*, New Jersey, A JOHN WILEY & SONS, INC., Ch. 2, 2007.

[14] S. Adachi, *Properties of Aluminium Gallium Arsenide*, London, INSPEC, the IEEE,1993.

[15] E.D. Palik, *Handbook of Optical Constants of Solids*, London, Academic press, 1998.

Seyed Peyman Abbasi was born in Tehran, Iran, in 1978. He received the M.S. degree in plasma physics from K.N. Toosi University of Technology in 2005. In 2019, he received the Ph.D. degree from Iran University of Science and Technology.

In 2006 he joined the Iranian National Laser Center. He was the head of the semiconductor laser group for 9 years. He currently leads the R&D section of semiconductor laser group. His main studies are on the laser diode structure, waveguide design and laser diode beam characterization.

Arash Hodaei was born in Tehran, Iran, in 1980. He received the B.S. degree in electronics engineering from Azad Tehran-Markaz University in 2003. In 2018, he received the M.S. degree from Tarbiat Modares University.

From 2004 to 2005, he was an R&D engineer in Raymond Computers Co. as a designer on various applicable projects. Then he joined the Rahrovan Sepehr Andisheh Co. as a senior production engineer in 2006. In 2008, he joined the semiconductor lasers group in Iranian National Laser Center. He now works in R&D Section. His specialty is laser diode simulation, characterization, and testing.